

## Antimicrobial properties and dental pulp stem cell cytotoxicity using carboxymethyl cellulose-silver nanoparticles deposited on titanium plates

Martha Alicia Laredo-Naranjo<sup>a</sup>, Roberto Carrillo-Gonzalez<sup>a</sup>, Myriam Angelica De La Garza-Ramos<sup>a,b</sup>, Marco Antonio Garza-Navarro<sup>c</sup>, Hilda H. H. Torre-Martinez<sup>a</sup>, Casiano Del Angel-Mosqueda<sup>b,d</sup>, Roberto Mercado-Hernandez<sup>a</sup> and Roberto Carrillo-Fuentevilla<sup>a</sup>

<sup>a</sup>Posgrado de Ortodoncia, Facultad de Odontología, Universidad Autónoma de Nuevo León, Monterrey, Mexico; <sup>b</sup>Centro de Investigación y Desarrollo en Ciencias de la Salud, Universidad Autónoma de Nuevo León, Monterrey, Mexico; <sup>c</sup>Centro de Innovación, Investigación y Desarrollo en Ingeniería y Tecnología, Facultad de Ingeniería Mecánica y Eléctrica, Universidad Autónoma de Nuevo León, Monterrey, Mexico; <sup>d</sup>Instituto de Biotecnología, Facultad de Ciencias Biológicas, Universidad Autónoma de Nuevo León, Monterrey, Mexico

### ABSTRACT

**Objective:** To evaluate the antimicrobial properties and dental pulp stem cells (DPSCs) cytotoxicity of synthesized carboxymethyl cellulose-silver nanoparticles impregnated on titanium plates. **Material and methods:** The antibacterial effect of silver nanoparticles in a carboxymethyl cellulose matrix impregnated on titanium plates (Ti-AgNPs) in three concentrations: 16%, 50% and 100% was determined by adding these to bacterial cultures of *Streptococcus mutans* and *Porphyromonas gingivalis*. The Ti-AgNPs cytotoxicity on DPSCs was determined using a fluorimetric cytotoxicity assay with 0.12% chlorhexidine as a positive control. **Results:** Silver nanoparticles in all concentrations were antimicrobial, with concentrations of 50% and 100% being more cytotoxic with 4% cell viability. Silver nanoparticles 16% had a cell viability of 95%, being less cytotoxic than 0.12% chlorhexidine. **Conclusions:** Silver nanoparticles are a promising structure because of their antimicrobial properties. These have high cell viability at a concentration of 16%, and are less toxic than chlorhexidine.

### ARTICLE HISTORY

Received 11 December 2015  
Revised 24 February 2016  
Accepted 29 February 2016

### KEYWORDS

Antibacterial activity; dental pulp stem cells; orthodontics



## Introduction

Silver nanoparticles (AgNPs) are a promising nanostructure because of their bactericidal, fungicidal and virucidal properties.[1,2] AgNPs have been widely used in personal care products, food services and as coatings for dental and medical instruments.[3–5] They have a remarkable bactericide activity against *Escherichia coli*, *Streptococcus pneumoniae*, *Staphylococcus aureus* and *Aspergillus niger*. [1,2] However, since AgNPs are mainly used in biomedical and health-care applications, their toxicity is a critical factor that must be considered. Yen et al. [6] documented that AgNPs less than 3 nm in size induce cytotoxicity in macrophages. Also, cell viability decreases in liver cells treated with AgNPs 15–100 nm in size.[7] This study suggests a dose-dependent effect related to AgNPs exposure.

Titanium mini-implants are used in orthodontics to obtain and improve skeletal anchorage. The placement of a mini-implant is simple, but contamination by

microorganisms can cause plaque formation and peri-implantitis which can result in epithelial infiltration, bleeding on probing, suppuration, bone loss, mobility, and mini-implant failure.[8–11] This failure is associated with the microbial flora traditionally involved in periodontitis, which are Gram-positive facultative anaerobes; however, a lack of oral hygiene can cause an increase in the number of Gram-negative bacteria.[12] The formation of plaque on the mini-implant is related to adhesion of *Streptococcus* spp which represent over 80% of primary colonizers; [13,14] secondary colonizers include *Aggregatibacter (Actinobacillus) actinomycetemcomitans*, *Prevotella intermedia*, *Treponema denticola* and *Porphyromonas gingivalis*. [5,15]

Nanotechnology offers the possibility of controlling the formation of oral biofilm through its unique attributes. Juan et al., [16] in China, deposited silver nanoparticles on a titanium surface and found that 94% of *Staphylococcus aureus* and 95% of *Escherichia coli* had been removed from the surface of the titanium

**CONTACT** Myriam Angelica de la Garza-Ramos  myriam.garzar@uanl.edu.mx  Facultad de Odontología, Universidad Autónoma de Nuevo León, Calle Dr. Eduardo Aguirre Pequeño s/n, Colonia Mitras Centro, Monterrey, Nuevo León, Mexico

© 2016 The Author(s). Published by Taylor & Francis. This is an Open Access article distributed under the terms of the Creative Commons Attribution-NonCommercial License (<http://creativecommons.org/licenses/by-nc/4.0/>), which permits unrestricted non-commercial use, distribution, and reproduction in any medium, provided the original work is properly cited.

implant. Similarly, Liao and Anchun [17] showed that a titanium surface modified with silver nanoparticles had good antibacterial properties as well as an absence of cytotoxicity when evaluated in human gingival fibroblasts. However, the benefits of using nano-sized products is challenged by concerns of toxicity, since little is known about the interaction between cells and nano-materials, including their mechanisms of absorption, distribution, toxicological parameters and mechanism of action.

In this study, we compared the bactericide and cytotoxicity capacity of synthesized AgNPs. For this, AgNPs were evaluated against *Streptococcus mutans* and *Porphyromonas gingivalis* and their cytotoxic effects on dental pulp stem cells (DPSCs) with AgNP-impregnated titanium surface, which represents dental mini-implants.

## Materials and methods

### Synthesis of AgNPs

A carboxymethyl cellulose (CMC) solution with silver nanoparticles with a total solid concentration of 6.06 mg/mL and a concentration of silver nanoparticles (AgNPs) of 0.06 mg/mL was acquired from the Center for Innovation and Development in Engineering and Technology of the Universidad Autonoma de Nuevo Leon.

The CMC–AgNPs composite was synthesized using a previously reported method with some modifications.[18,19] Briefly, aqueous CMC and silver nitrate solutions were prepared at concentrations of 15 and 0.95 mg/mL, respectively, using deionized water. Then, 20 mL of CMC was poured at room temperature into a round-bottom three-neck flask and stirred for 10 min. Later, 10 mL of silver nitrate solution was added to the reactor and the temperature was quickly raised to 90 °C. The reaction was kept at this temperature for 24 h under reflux conditions. Once the reaction time had elapsed, the resultant yellowish solution was rapidly poured into a previously cooled round-bottom flask in order to cool it to room temperature. This solution was frozen in the flask and then lyophilized. A dried sample was weighted and finally dissolved in deionized water to obtain a CMC–AgNP solution with a concentration of 0.06 mg/mL. Later, it was demonstrated that the silver ions were totally reduced into Ag<sup>0</sup>; hence the weight ratio of CMC/AgNPs in the composite can be calculated as 50.

The crystalline and morphological features of the CMC–AgNPs composite were examined by transmission electron microscopy (TEM) in a field emission

gun, FEI Titan G 2 80–300 microscope (FEI Co., Hillsboro, OR) using bright field (BF) and Z-contrast (HAADF-STEM) imaging as well as selected area electron diffraction (SAED). Particle size distribution of AgNPs was obtained by measuring at least 300 randomly selected particles. Ultraviolet-visible (UV–vis) spectroscopy studies of the CMC–AgNPs composite as well as AgNO<sub>3</sub> precursor solution were performed in a Perkin-Elmer, Lambda 35, spectrometer (PerkinElmer, Inc., Waltham, MA). Fourier transform infrared spectroscopy (FTIR) analysis of pure CMC as well as CMC–AgNPs composite was recorded from a Z Nicolet 6700 spectrometer (Thermo Electron Corporation, Madison, WI).

### AgNPs composite coating of titanium plates

Twenty-two titanium-vanadium plates 9 mm in diameter and 2 mm thick were used for this study; of these, 18 sterile plates were taken and divided into three subgroups of six titanium discs. The titanium discs were coated with three different aqueous dissolutions of the CMC–AgNPs composite prepared at concentrations of AgNPs of 0.06, 0.03 or  $9.6 \times 10^{-3}$  mg/mL. Then, 200 mL of each dissolution was poured over the plates of each of the subgroups. The plates were then placed in an oven at 60 °C for 24 h, in order to evaporate the dissolvent and obtain the composite coating on the titanium plates. The coating of the Ti plates was analyzed with a scanning electron microscope (SEM) using a backscattered electrons imaging technique in a FEI FEG Nova NanoSEM (FEI Company, Hillsboro, OR).

### Antibacterial testing of AgNPs

The antimicrobial activity of the different concentrations of AgNPs on the titanium plates was tested with the Gram-negative bacterium, *Porphyromonas gingivalis* strain W83 (ATCC BAA-308) and the Gram-positive bacterium, *Streptococcus mutans* strain UA159 (ATCC 700610). Nine plates with tryptone soy for *S. mutans* and nine blood agar plates for *P. gingivalis* were inoculated by diffusion with 1 mL of the bacterial strains achieving a homogeneous layer. Following this, the titanium plates coated with the different concentrations of AgNPs were individually placed. Subsequently, they were incubated at 37 °C for 16 h and finally, the inhibition zone was measured. This procedure was repeated three times per concentration. A plate without AgNPs was used as a negative control, and a disc impregnated with chlorhexidine 0.12% was used as a positive control. A total of 20 titanium discs were

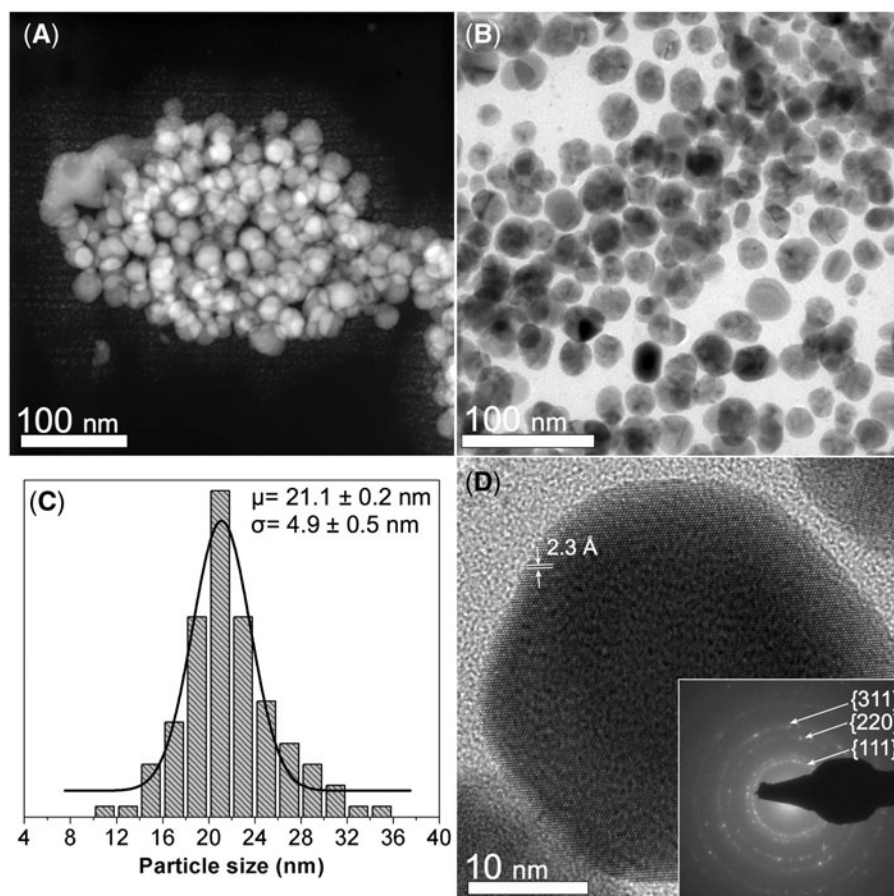


**Figure 1.** Morphological and crystalline characterization of the synthesized CMC-AgNPs composite. (A) A HAADF-STEM image showing several nanoparticles (brighter zones) that are grouped in the CMC matrix (darker background). (B) A BF image where the quasi-spherical morphology of the nanoparticles can be observed. (C) Particle size distribution of the composite. (D) The nanoparticles display a regular atomic arrangement that is congruent with that reported for family planes {111} of silver crystalline structure, having a regular spacing of 2.3 Å (JCPDS: 04–0783). SAED pattern obtained from the zone shown in B confirms the crystalline structure of the nanoparticles (inset Figure 1D).

used, 18 with AgNPs, 1 without AgNPs, and 1 with 0.12% chlorhexidine.

#### Cell culture and fluorimetric cytotoxicity assay

DPSCs were used for cytotoxicity testing. The toxicity of AgNPs was tested on DPSCs cultivated in  $\alpha$ -modified Eagle's medium ( $\alpha$ -MEM) supplemented with 10% fetal bovine serum (FBS) (Gibco-Invitrogen, Carlsbad, CA), 2 mM L-glutamine, 100 U/ml penicillin, 100  $\mu$ g/ml streptomycin and 0.25  $\mu$ g/ml amphotericin B (Sigma-Aldrich Corporation, St. Louis, MO) at 37 °C in a humidified atmosphere with 5% CO<sub>2</sub>. [20] After obtaining cell confluence, 15 000 cells per well were seeded onto 96-well black plates, maintaining these in growth medium for 24 h (Corning Inc., Corning, NY). AgNPs were added at concentrations of 100%, 50% and 16%. PBS was used as a negative control and 0.12% chlorhexidine as a positive control. After 24 h incubation, the medium was removed and the cells were washed three times with PBS.

The cytotoxicity assay was performed as described by Larsson and Nygren.[21] Briefly, fluorescein diacetate (FDA, Sigma-Aldrich Co., St. Louis, MO) was dissolved in DMSO (Sigma-Aldrich) and kept frozen at –20 °C as a stock solution (10 mg/mL). FDA was diluted in PBS at 10  $\mu$ g/mL and 200  $\mu$ L was added to each well. The plates were then incubated for 30 min at 37 °C in the dark. A 96-well scanning fluorometer GloMax<sup>®</sup> Multi + Microplate Multimode (Promega, Madison, WI) was used at 495 nm. Data were analyzed to determine cell viability (%).

#### Statistical analysis

Each group was compared using an independent Student's *t* test with a 95% confidence interval, considering a *p* values  $\leq 0.05$  as statistically significant. Similarly, ANOVA and the Tukey test were performed for both cytotoxicity and antimicrobial tests using a 95% confidence interval so that *p* values  $< 0.01$  were

considered statistically significant. Each assay was performed in triplicate.

## Results

### Crystalline and morphological characterization of CMC-AgNPs composite

Figure 1 shows the morphological and crystalline characterization of the synthesized CMC-AgNPs composite. Figure 1A shows a HAADF-STEM image where several nanoparticles (brighter zones) grouped in the CMC matrix (darker background) are seen. Figure 1B displays a BF image where the quasi-spherical morphology of the nanoparticles is seen. The particle size distribution in the composite is shown in Figure 1C. The particles have a center of 21.1 nm and a standard deviation of 4.9 nm. In Figure 1D, the nanoparticles display a regular atomic arrangement that is congruent

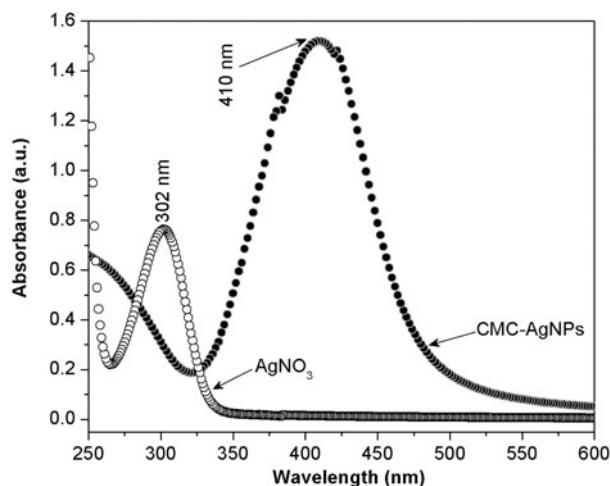


**Figure 2.** The spectrum obtained from CMC-AgNPs composite does not show an absorption band that agrees with that observed at 301 nm in the spectrum of  $\text{AgNO}_3$  reagent, but it shows a well defined band around 400 nm that is congruent with the surface plasmon resonance phenomenon reported for silver nanoparticles.

with that reported for family planes  $\{111\}$  of silver crystalline structure, having a regular spacing of 2.3 Å (JCPDS: 04-0783). The SAED pattern obtained from the zone shown in B confirms the crystalline structure of the nanoparticles (see inset in Figure 1D), since we can recognize diffraction rings related to the family planes  $\{111\}$ ,  $\{220\}$  and  $\{311\}$  reported for FCC packing of silver (JCPDS: 04-0783).

Accordingly, we proceeded to corroborate that  $\text{Ag}^+$  was fully reduced using the UV-vis spectroscopy technique. Hence, we measured the spectra of the as-prepared CMC-AgNPs composite as well as of the aqueous  $\text{AgNO}_3$  dissolution used for its synthesis. As shown in Figure 2, the spectrum obtained from CMC-AgNPs composite does not show an absorption band that agrees with that observed at 301 nm in the spectrum of  $\text{AgNO}_3$  reagent; but it shows a well-defined band around 400 nm that is congruent with the surface plasmon resonance phenomenon reported for silver nanoparticles.[22] This result suggests the full reduction of the added  $\text{Ag}^+$  into  $\text{Ag}^0$ ; hence, CMC/AgNPs weight ratio in the composite can be calculated as 50.

### Morphological characterization of composite coating

Figure 3 shows SEM images obtained at different magnifications from one of the coated Ti plates using the back scattering electron technique. Herein is shown a low magnification image where the composite coating (dark zone) is observed on the Ti plate (brighter background) (Figure 3A). Figure 3B displays the manner that AgNPs (brighter dots) are dispersed in the CMC matrix (darker background), which is added to the plate. In addition, Figure 3C shows at 160 kX, the morphology of the AgNPs, which agrees with that obtained from TEM characterization of the composite.

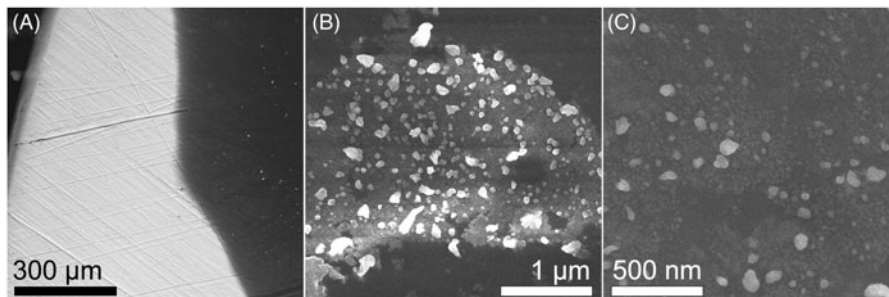


**Figure 3.** SEM images obtained at different magnifications from one of the coated Ti plates using BSE technique. (A) A low magnification image shows the composite coating (dark zone) on the Ti plate (brighter background). (B) AgNPs (brighter dots) are dispersed in the CMC matrix (darker background). (C) Shows the morphology of the AgNPs at 160 kX, which agrees with that obtained from TEM characterization of the composite.



## Antimicrobial Activity

A greater inhibitory effect was observed with *P. gingivalis* than with *S. mutans* (Table 1). Similarly, a greater bacterial inhibition was seen with both bacteria as the concentration of AgNPs increased, with larger inhibition halos being seen with the concentration of 100%, followed by 50% and 16% (Table 1). A statistically significant difference between the inhibition zones of the three silver nanoparticle concentrations was also found ( $P = 0.004$ ).

When the different results of the AgNPs concentrations were compared using Student's *t* test, we found greater bacterial inhibition at a concentration of 50% compared to 16%, with a statistically significant difference ( $p = 0.0132$ ). A greater area of inhibition was also found at a concentration of 100% compared to 16% with a statistically significant difference ( $p = 0.0074$ ). When the concentrations of 50% and 100% were compared, a greater inhibition zone was seen with the latter ( $p = 0.0074$ ).

However, with the Tukey test, no statistically significant difference was found between the concentrations of 5% and 100% with *S. mutans* ( $p = 0.151$ ) (Table 2). A significant difference was found in the inhibition diameters with the different concentrations with regard to *P. gingivalis* ( $p = 0.000$ ). This was also corroborated by the Tukey test (Table 2).

When the results between the different concentrations of AgNPs were compared using Student's *t* test, increased bacterial inhibition was found at a

**Table 1.** Diameter of inhibition zone with AgNPs, chlorhexidine and a negative control.

Solutions	Zone diameters	
	<i>S. mutans</i>	<i>P. gingivalis</i>
AgNPs concentration		
16%	1.083 (0.02)	1.13 (0.02)
50%	1.183 (0.02)	1.35 (0.05)
100%	1.25 (0.05)	1.62 (0.02)
Chlorhexidine 0.12%	1.7	2.3
Negative control	1	1

Data are shown in mm as means and standard deviation (SD). Diameter of inhibition zone was measured in mm with a digital Vernier caliper.

**Table 2.** Tukey test of antimicrobial effect on *S. mutans* and *P. gingivalis* with three different AgNPs concentrations (16, 50, and 100%).

Concentration (%)	N	Mean	Standard deviation	Typical error	95% Confidence Interval			
					Lower bound	Upper bound	Min	Max
<i>S. mutans</i>								
16	3	1.0833	0.02687	0.01667	1.0116	1.1550	1.05	1.10
50	3	1.1833	0.02887	0.01667	1.1116	1.2550	1.15	1.20
100	3	1.2500	0.05000	0.02887	1.1258	1.3742	1.20	1.30
Total	9	1.1722	0.07949	0.02650	1.1111	1.2333	1.05	1.30
<i>P. gingivalis</i>								
16	3	1.1333	0.02887	0.01667	1.0616	1.2050	1.10	1.15
50	3	1.3500	0.05000	0.02887	1.2258	1.4742	1.30	1.40
100	3	1.6267	0.02517	0.01453	1.5642	1.6892	1.60	1.65
Total	9	1.3700	0.21645	0.07215	1.2036	1.5364	1.10	1.65

concentration of 50% compared to 16%, with a statistically significant difference ( $p = 0.0028$ ). Likewise, a larger inhibition zone was found with the concentration of 100% compared to 16% with this not being statistically significant ( $p = 2.389$ ). Finally, when the concentrations of 50–100% were compared, a larger diameter of inhibition was observed with the latter; however, no statistically significant difference was found ( $p = 0.9480$ ).

When the results of different concentrations of AgNPs were compared with chlorhexidine 0.12%, it was found that the latter produces a much larger bacterial inhibition halo for both *S. mutans* and *P. gingivalis*.

## Cytotoxicity

A significant reduction in the number of cells at a concentration of 100% was found since only 4% were viable (Figure 4). These results are similar to the concentration of 50%, which resulted in 3.99% viable cells. However, no significant reduction in cell viability was found with the concentration of 16%, which had 95% viable cells. In contrast, chlorhexidine 0.12% presented a viability of 62% (Figure 4). A statistically significant difference in cytotoxicity was not found between the nanoparticle concentrations of 50 and 100% ( $p = 0.995$ ).

## Discussion

The AgNPs-titanium plate had antibacterial properties at different concentrations with greater affinity of AgNPs for Gram-negative bacteria (*P.s. gingivalis*). This may be because Gram-positive bacteria contain 3–20 times more peptidoglycan than Gram-negative bacteria. This polymer has a negative charge and probably blocks a portion of silver ions, limiting the penetration of AgNPs; consequently, Gram-positive bacteria are less susceptible.[23,24] There are studies with *S. aureus*

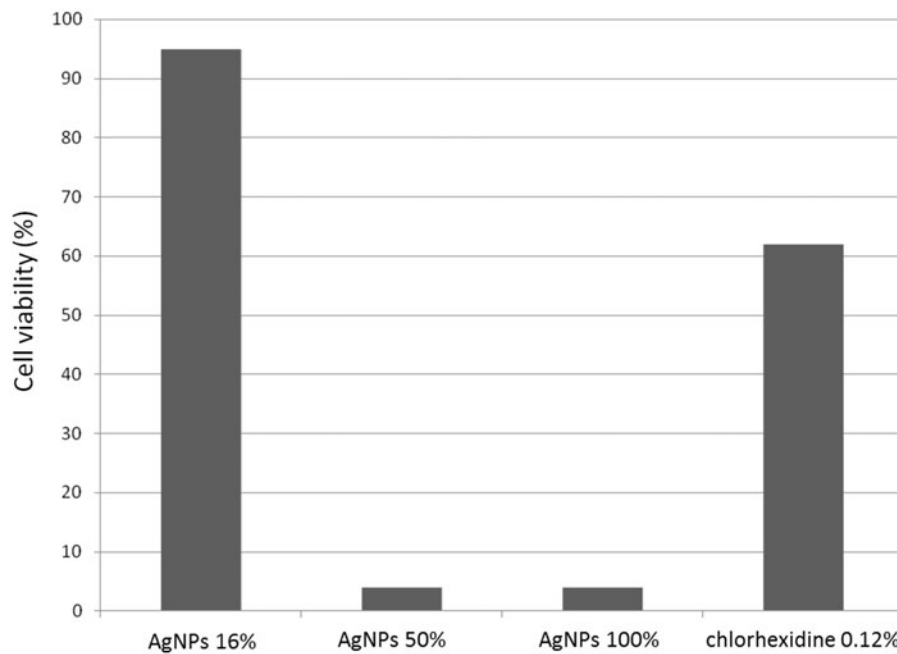


**Figure 4.** Viability of dental pulp stem cells (DPSC) with different concentrations of AgNPs and chlorhexidine 0.12%.

(Gram-positive) and *E. coli* (Gram-negative) that are consistent with this study, with increased susceptibility of Gram-negative bacteria.[17,25]

Gram-negative anaerobic bacteria have also been found to be more susceptible to chlorhexidine with a greater affinity for *P. gingivalis* and *Prevotella nigrescens*, followed by *S. mutans* and *S. sanguis*. [26] This affinity was observed in this study, together with superior antimicrobial properties of chlorhexidine 0.12% compared with any concentration of AgNPs. Greater antimicrobial properties have been found with greater concentrations of AgNPs, noting that the zone of inhibition increased as the concentration increased.[25] However, other studies [1,27] mention an inverse relationship between the size of AgNPs and their antimicrobial activity. Morones [1] reported that AgNPs particles in the range of 1 to 10 nm have greater antimicrobial activity. In this study, we used AgNPs with a size of 21.1 nm and a standard deviation of 4.9 nm. This is a nanoparticle size greater than that reported by Morones. AgNPs interact with the cell surface of bacteria adhering and accumulating on the surface of the bacterial cell membrane causing structural changes that make bacteria more permeable, a condition that is influenced by the nanoparticles' size, shape and concentration. Smaller nanoparticles seem to have a greater ability to penetrate bacteria.[28] In this study, the inhibition zone of both bacterial strains was below that of 0.12% chlorhexidine. Chlorhexidine was used as a control because it is an effective plaque-inhibiting solution that has been extensively tested.

Monteiro [23] examined the toxicity of AgNPs at a concentration of 5  $\mu\text{g}$  Ag/mL in spermatogonial stem cells, observing that they induce necrosis or apoptosis of these cells. This may explain the results found in this study where cytotoxicity increased at concentrations of 50–100%, equivalent to 6.06  $\mu\text{g}/\text{mL}$  and 12.12  $\mu\text{g}/\text{mL}$ , respectively. These concentrations are greater than the amount mentioned by Monteiro as toxic (5  $\mu\text{g}/\text{mL}$ ). Nanoparticles 16% showed no cytotoxicity because their concentration (1.92  $\mu\text{g}/\text{mL}$ ) is below the amount mentioned.

Liu [27] stated that silver nanoparticles with a smaller size and a higher concentration showed greater cytotoxicity and a greater antimicrobial effect. This is consistent with this research, in which a relationship between nanoparticle concentration and size and cytotoxicity and antimicrobial effect was found.

Other studies have been conducted to evaluate the cytotoxicity of AgNPs in various cells such as human gingival fibroblasts. These showed that cell morphology was not affected by a titanium surface with AgNPs [16]. This is consistent with our study where a low toxicity on DPSCs was observed at a low concentration of AgNPs (16%).

Furthermore, in our study, there was no statistically significant difference between the results of AgNPs concentrations of 50 and 100%, either in their antimicrobial or cytotoxicity results. This makes us consider that cells are saturated with silver nanoparticles at a concentration of 50%. Receptors cannot bind more substrate, i.e. nanoparticles, which explain the

reason for the similarity of results in cytotoxicity testing. This also occurs in antimicrobial testing.

Our results show that AgNPs have good antimicrobial properties with high cell viability at a concentration of 16% making this a viable choice as a coating on dental implants. It is important to obtain non-toxic materials that are capable of producing a sustained targeted release of antibacterial silver at the implantation site; however, this requires further investigation to determine possible interactions in living beings since not much is known about their mechanism of action, absorption, distribution, and toxic properties. Unlike other reports, the aforementioned composite was synthesized following a totally ecofriendly approach that does not use or produce any harmful residue. Also, the evaluation of cytotoxicity in DPSCs using silver nanoparticles synthesized using this method is novel.

## Conclusions

AgNP coating on a titanium plate has an anti-microbial effect against *P. gingivalis* and *S. mutans* especially at higher concentrations. Low cytotoxicity of silver nanoparticles occurs at a concentration of 16% with 95% viability of DPSCs; however, cytotoxicity exists at concentrations above 50%.

Chlorhexidine was more cytotoxic than AgNP at a lower concentration; similarly 0.12% chlorhexidine has a greater antimicrobial effect than any concentration of silver nanoparticles. Knowing these properties, we can provide a solution that increases fibro-integration of dental mini-implants in orthodontic treatments.

## Acknowledgements

The authors thank Sergio Lozano-Rodriguez, M.D., for his help in translating and editing the manuscript.

## Disclosure statement

The authors declare that they received no funding for this research.

## References

- [1] Morones JR, Elechiguerra JL, Camacho A, et al. The bactericidal effect of silver nanoparticles. *Nanotechnology*. 2005;16:2346–2353.
- [2] Lara HH, Garza-Trevino EN, Ixtapan-Turrent L, et al. Silver nanoparticles are broad-spectrum bactericidal and virucidal compounds. *J Nanobiotechnology*. 2011;9:30
- [3] Park EJ, Yi J, Kim Y, et al. Silver nanoparticles induce cytotoxicity by a Trojan-horse type mechanism. *Toxicol in Vitro*. 2010;24:872–878.
- [4] Wijnhoven S. Human health risk assessment of nano-silver. Overview of available data [Internet]. BfR conference on nanosilver. Berlin: Federal Institute for Risk Assessment (BfR); 2012 [cited 2015 Nov 2]. Available from: <http://www.bfr.bund.de/cm/349/human-health-risk-assessment-of-nanosilver.pdf>
- [5] Allaker R. The use of nanoparticles to control oral biofilm formation. *J Dent Res*. 2010;89:1175–1186.
- [6] Yen HJ, Hsu SH, Tsai CL. Cytotoxicity and immunological response of gold and silver nanoparticles of different sizes. *Small*. 2009;5:1553–1561.
- [7] Hussain SM, Hess KL, Gearhart JM, et al. In vitro toxicity of nanoparticles in BRL 3A rat liver cells. *Toxicol in Vitro*. 2005;19:975–983.
- [8] de Freitas AO, Alviano CS, Alviano DS, et al. Microbial colonization in orthodontic mini-implants. *Braz Dent J*. 2012;23:422–427.
- [9] Quinteros Borgarello M, Delgado Molina E, Sánchez Garcés M, et al. Estudio microbiológico de la periimplantitis: Presentación de 9 casos clínicos. *Av Periodon Implantol*. 2000;12:137–150.
- [10] Mombelli A. Microbiology and antimicrobial therapy of peri-implantitis. *Periodontol*. 2002;28:177–189.
- [11] Pye AD, Lockhart DE, Dawson MP, et al. A review of dental implants and infection. *J Hosp Infect*. 2009;72:104–110.
- [12] Avila M, Ojcius DM, Yilmaz O. The oral microbiota: living with a permanent guest. *DNA Cell Biol*. 2009;28:405–411.
- [13] Rodríguez Hernández AG. Estudio de la interacción de bacterias implicadas en la formulación de placa dentro-bacteriana con superficies de titanio comercialmente puro in vitro y su asociación con la periimplantitis. 2009. Doctoral thesis. Available from: <http://hdl.handle.net/10803/6068>.
- [14] Subramani K, Jung RE, Molenberg A, et al. Biofilm on dental implants: a review of the literature. *Int J Oral Maxillofac Implants*. 2008;24:616–626.
- [15] Brogden KA, Guthmiller JM. Periodontal diseases. In: Brogden KA, Guthmiller JM, editors. *Polymicrobial diseases*. Washington (DC): ASM Press; 2002. Available at: <http://www.ncbi.nlm.nih.gov/books/NBK2496/>
- [16] Juan L, Zhimin Z, Anchun M, et al. Deposition of silver nanoparticles on titanium surface for antibacterial effect. *Int J Nanomedicine*. 2010;5:261–267.
- [17] Liao J, Anchun M, Zhu Z, et al. Antibacterial titanium plate deposited by silver nanoparticles exhibits cell compatibility. *Int J Nanomedicine*. 2010;5:337–342.
- [18] Garza-Navarro MA, Aguirre-Rosales JA, Llanas-Vázquez EE, et al. Totally ecofriendly synthesis of silver nanoparticles from aqueous dissolutions of polysaccharides. *Int J Polym Sci*. 2013; 2013:436021.
- [19] Martínez-Rodríguez MA, Garza-Navarro MA, Moreno-Cortez IE, et al. Silver/polysaccharide-based nanofibrous materials synthesized from green chemistry approach. *Carbohydr Polym*. 2016;136:46–53.
- [20] Del Angel-Mosqueda C, Gutierrez-Puente Y, Lopez-Lozano AP, et al. Epidermal growth factor enhances osteogenic differentiation of dental pulp stem cells in vitro. *Head Face Med*. 2015;11:29.

- [21] Larsson R, Nygren P. A rapid fluorometric method for semiautomated determination of cytotoxicity and cellular proliferation of human tumor cell lines in microculture. *Anticancer Res.* 1989;9:1111–1119.
- [22] Kemp MM, Kumar A, Mousa S, et al. Synthesis of gold and silver nanoparticles stabilized with glycosaminoglycans having distinctive biological activities. *Biomacromolecules.* 2009;10:589–595.
- [23] Monteiro DR, Gorup LF, Takamiya AS, et al. The growing importance of materials that prevent microbial adhesion: antimicrobial effect of medical devices containing silver. *Int J Antimicrob Agents.* 2009;34:103–110.
- [24] García-Contreras R, Argueta-Figueroa L, Mejía-Rubalcava C, et al. Perspectives for the use of silver nanoparticles in dental practice. *Int Dent J.* 2011;61:297–301.
- [25] Madhumathi K, Sudheesh Kumar PT, Abhilash S, et al. Development of novel chitin/nanosilver composite scaffolds for wound dressing applications. *J Mater Sci Mater Med.* 2010;21:807–813.
- [26] McBain AJ, Bartolo RG, Catrenich CE, et al. Effects of a chlorhexidine gluconate-containing mouthwash on the vitality and antimicrobial susceptibility of in vitro oral bacterial ecosystems. *Appl Environ Microbiol.* 2003;69:4770–4776.
- [27] Liu H-L, Dai SA, Fu K-Y, et al. Antibacterial properties of silver nanoparticles in three different sizes and their nanocomposites with a new waterborne polyurethane. *Int J Nanomedicine.* 2010;5:1017–1028
- [28] Franci G, Falanga A, Galdiero S, et al. Silver nanoparticles as potential antibacterial agents. *Molecules.* 2015;20:8856–8874.